

## Inclusive cross section and double helicity asymmetry for $\pi^0$ production in $p + p$ collisions at $\sqrt{s} = 200$ GeV: Implications for the polarized gluon distribution in the proton

A. Adare,<sup>8</sup> S. Afanasiev,<sup>22</sup> C. Aidala,<sup>9</sup> N. N. Ajitanand,<sup>48</sup> Y. Akiba,<sup>42,43</sup> H. Al-Bataineh,<sup>37</sup> J. Alexander,<sup>48</sup> K. Aoki,<sup>27,42</sup> L. Aphecetche,<sup>50</sup> R. Armendariz,<sup>37</sup> S. H. Aronson,<sup>3</sup> J. Asai,<sup>43</sup> E. T. Atomssa,<sup>28</sup> R. Averbeck,<sup>49</sup> T. C. Awes,<sup>38</sup> B. Azmoun,<sup>3</sup> V. Babintsev,<sup>18</sup> G. Baksay,<sup>14</sup> L. Baksay,<sup>14</sup> A. Baldisseri,<sup>11</sup> K. N. Barish,<sup>4</sup> P. D. Barnes,<sup>30</sup> B. Bassalleck,<sup>36</sup> S. Bathe,<sup>4</sup> S. Batsouli,<sup>38</sup> V. Baublis,<sup>41</sup> A. Bazilevsky,<sup>3</sup> S. Belikov,<sup>3</sup> R. Bennett,<sup>49</sup> Y. Berdnikov,<sup>45</sup> A. A. Bickley,<sup>8</sup> J. G. Boissevain,<sup>30</sup> H. Borel,<sup>11</sup> K. Boyle,<sup>49</sup> M. L. Brooks,<sup>30</sup> H. Buesching,<sup>3</sup> V. Bumazhnov,<sup>18</sup> G. Bunce,<sup>3,43</sup> S. Butsyk,<sup>30,49</sup> S. Campbell,<sup>49</sup> B. S. Chang,<sup>57</sup> J.-L. Charvet,<sup>11</sup> S. Chernichenko,<sup>18</sup> J. Chiba,<sup>23</sup> C. Y. Chi,<sup>9</sup> M. Chiu,<sup>19</sup> I. J. Choi,<sup>57</sup> T. Chujo,<sup>54</sup> P. Chung,<sup>48</sup> A. Churny,<sup>18</sup> V. Cianciolo,<sup>38</sup> C. R. Clevén,<sup>16</sup> B. A. Cole,<sup>9</sup> M. P. Comets,<sup>39</sup> P. Constantin,<sup>30</sup> M. Csanád,<sup>13</sup> T. Csörgő,<sup>24</sup> T. Dahms,<sup>49</sup> K. Das,<sup>15</sup> G. David,<sup>3</sup> M. B. Deaton,<sup>1</sup> K. Dehmelt,<sup>14</sup> H. Delagrangé,<sup>50</sup> A. Denisov,<sup>18</sup> D. d'Enterria,<sup>9</sup> A. Deshpande,<sup>43,49</sup> E. J. Desmond,<sup>3</sup> O. Dietzsch,<sup>46</sup> A. Dion,<sup>49</sup> M. Donadelli,<sup>46</sup> O. Drapier,<sup>28</sup> A. Drees,<sup>49</sup> A. K. Dubey,<sup>56</sup> A. Durum,<sup>18</sup> V. Dzhordzhadze,<sup>4</sup> Y. V. Efremenko,<sup>38</sup> J. Egdemir,<sup>49</sup> F. Ellinghaus,<sup>8</sup> W. S. Emam,<sup>4</sup> A. Enokizono,<sup>29</sup> H. En'yo,<sup>42,43</sup> S. Esumi,<sup>53</sup> K. O. Eyser,<sup>4</sup> D. E. Fields,<sup>36,43</sup> M. Finger,<sup>5,22</sup> M. Finger, Jr.,<sup>5,22</sup> F. Fleuret,<sup>28</sup> S. L. Fokin,<sup>26</sup> Z. Fraenkel,<sup>56</sup> J. E. Frantz,<sup>49</sup> A. Franz,<sup>3</sup> A. D. Frawley,<sup>15</sup> K. Fujiwara,<sup>42</sup> Y. Fukao,<sup>27,42</sup> T. Fusayasu,<sup>35</sup> S. Gadrat,<sup>31</sup> I. Garishvili,<sup>51</sup> A. Glenn,<sup>8</sup> H. Gong,<sup>49</sup> M. Gonin,<sup>28</sup> J. Gosset,<sup>11</sup> Y. Goto,<sup>42,43</sup> R. Granier de Cassagnac,<sup>28</sup> N. Grau,<sup>21</sup> S. V. Greene,<sup>54</sup> M. Grosse Perdekamp,<sup>19,43</sup> T. Gunji,<sup>7</sup> H.-Å. Gustafsson,<sup>32</sup> T. Hachiya,<sup>17</sup> A. Hadj Henni,<sup>50</sup> C. Haegemann,<sup>36</sup> J. S. Haggerty,<sup>3</sup> H. Hamagaki,<sup>7</sup> R. Han,<sup>40</sup> H. Harada,<sup>17</sup> E. P. Hartouni,<sup>29</sup> K. Haruna,<sup>17</sup> E. Haslum,<sup>32</sup> R. Hayano,<sup>7</sup> M. Heffner,<sup>29</sup> T. K. Hemmick,<sup>49</sup> T. Hester,<sup>4</sup> X. He,<sup>16</sup> H. Hiejima,<sup>19</sup> J. C. Hill,<sup>21</sup> R. Hobbs,<sup>36</sup> M. Hohmann,<sup>14</sup> W. Holzmann,<sup>48</sup> K. Homma,<sup>17</sup> B. Hong,<sup>25</sup> T. Horaguchi,<sup>42,52</sup> D. Hornback,<sup>51</sup> T. Ichihara,<sup>42,43</sup> K. Imai,<sup>27,42</sup> M. Inaba,<sup>53</sup> Y. Inoue,<sup>44,42</sup> D. Isenhower,<sup>1</sup> L. Isenhower,<sup>1</sup> M. Ishihara,<sup>42</sup> T. Isobe,<sup>7</sup> M. Issah,<sup>48</sup> A. Isupov,<sup>22</sup> B. V. Jacak,<sup>49,\*</sup> J. Jia,<sup>9</sup> J. Jin,<sup>9</sup> O. Jinnouchi,<sup>43</sup> B. M. Johnson,<sup>3</sup> K. S. Joo,<sup>34</sup> D. Jouan,<sup>39</sup> F. Kajihara,<sup>7</sup> S. Kametani,<sup>7,55</sup> N. Kamihara,<sup>42</sup> J. Kamin,<sup>49</sup> M. Kaneta,<sup>43</sup> J. H. Kang,<sup>57</sup> H. Kanou,<sup>42,52</sup> D. Kawall,<sup>43</sup> A. V. Kazantsev,<sup>26</sup> A. Khanzadeev,<sup>41</sup> J. Kikuchi,<sup>55</sup> D. H. Kim,<sup>34</sup> D. J. Kim,<sup>57</sup> E. Kim,<sup>47</sup> E. Kinney,<sup>8</sup> A. Kiss,<sup>13</sup> E. Kistenev,<sup>3</sup> A. Kiyomichi,<sup>42</sup> J. Klay,<sup>29</sup> C. Klein-Boesing,<sup>33</sup> L. Kochenda,<sup>41</sup> V. Kochetkov,<sup>18</sup> B. Komkov,<sup>41</sup> M. Konno,<sup>53</sup> D. Kotchetkov,<sup>4</sup> A. Kozlov,<sup>56</sup> A. Král,<sup>10</sup> A. Kravitz,<sup>9</sup> J. Kubart,<sup>5,20</sup> G. J. Kunde,<sup>30</sup> N. Kurihara,<sup>7</sup> K. Kurita,<sup>44,42</sup> M. J. Kweon,<sup>25</sup> Y. Kwon,<sup>51,57</sup> G. S. Kyle,<sup>37</sup> R. Lacey,<sup>48</sup> Y.-S. Lai,<sup>9</sup> J. G. Lajoie,<sup>21</sup> A. Lebedev,<sup>21</sup> D. M. Lee,<sup>30</sup> M. K. Lee,<sup>57</sup> T. Lee,<sup>47</sup> M. J. Leitch,<sup>30</sup> M. A. L. Leite,<sup>46</sup> B. Lenzi,<sup>46</sup> T. Liška,<sup>10</sup> A. Litvinenko,<sup>22</sup> M. X. Liu,<sup>30</sup> X. Li,<sup>6</sup> B. Love,<sup>54</sup> D. Lynch,<sup>3</sup> C. F. Maguire,<sup>54</sup> Y. I. Makdisi,<sup>3</sup> A. Malakhov,<sup>22</sup> M. D. Malik,<sup>36</sup> V. I. Manko,<sup>26</sup> Y. Mao,<sup>40,42</sup> L. Mašek,<sup>5,20</sup> H. Masui,<sup>53</sup> F. Matathias,<sup>9</sup> M. McCumber,<sup>49</sup> P. L. McGaughey,<sup>30</sup> Y. Miake,<sup>53</sup> P. Mikeš,<sup>5,20</sup> K. Miki,<sup>53</sup> T. E. Miller,<sup>54</sup> A. Milov,<sup>49</sup> S. Mioduszewski,<sup>3</sup> M. Mishra,<sup>2</sup> J. T. Mitchell,<sup>3</sup> M. Mitrovski,<sup>48</sup> A. Morreale,<sup>4</sup> D. P. Morrison,<sup>3</sup> T. V. Moukhanova,<sup>26</sup> D. Mukhopadhyay,<sup>54</sup> J. Murata,<sup>44,42</sup> S. Nagamiya,<sup>23</sup> Y. Nagata,<sup>53</sup> J. L. Nagle,<sup>8</sup> M. Naglis,<sup>56</sup> I. Nakagawa,<sup>42,43</sup> Y. Nakamiya,<sup>17</sup> T. Nakamura,<sup>17</sup> K. Nakano,<sup>42,52</sup> J. Newby,<sup>29</sup> M. Nguyen,<sup>49</sup> B. E. Norman,<sup>30</sup> A. S. Nyanin,<sup>26</sup> E. O'Brien,<sup>3</sup> S. X. Oda,<sup>7</sup> C. A. Ogilvie,<sup>21</sup> H. Ohnishi,<sup>42</sup> H. Okada,<sup>27,42</sup> K. Okada,<sup>43</sup> M. Oka,<sup>53</sup> O. O. Omiwade,<sup>1</sup> A. Oskarsson,<sup>32</sup> M. Ouchida,<sup>17</sup> K. Ozawa,<sup>7</sup> R. Pak,<sup>3</sup> D. Pal,<sup>54</sup> A. P. T. Palounek,<sup>30</sup> V. Pantuev,<sup>49</sup> V. Papavassiliou,<sup>37</sup> J. Park,<sup>47</sup> W. J. Park,<sup>25</sup> S. F. Pate,<sup>37</sup> H. Pei,<sup>21</sup> J.-C. Peng,<sup>19</sup> H. Pereira,<sup>11</sup> V. Peresedov,<sup>22</sup> D. Yu. Peressounko,<sup>26</sup> C. Pinkenburg,<sup>3</sup> M. L. Purschke,<sup>3</sup> A. K. Purwar,<sup>30</sup> H. Qu,<sup>16</sup> J. Rak,<sup>36</sup> A. Rakotozafindrabe,<sup>28</sup> I. Ravinovich,<sup>56</sup> K. F. Read,<sup>38,51</sup> S. Rembeczki,<sup>14</sup> M. Reuter,<sup>49</sup> K. Reygers,<sup>33</sup> V. Riabov,<sup>41</sup> Y. Riabov,<sup>41</sup> G. Roche,<sup>31</sup> A. Romana,<sup>28,†</sup> M. Rosati,<sup>21</sup> S. S. E. Rosendahl,<sup>32</sup> P. Rosnet,<sup>31</sup> P. Rukoyatkin,<sup>22</sup> V. L. Rykov,<sup>42</sup> B. Sahlmueller,<sup>33</sup> N. Saito,<sup>27,42,43</sup> T. Sakaguchi,<sup>3</sup> S. Sakai,<sup>53</sup> H. Sakata,<sup>17</sup> V. Samsonov,<sup>41</sup> S. Sato,<sup>23</sup> S. Sawada,<sup>23</sup> J. Seele,<sup>8</sup> R. Seidl,<sup>19</sup> V. Semenov,<sup>18</sup> R. Seto,<sup>4</sup> D. Sharma,<sup>56</sup> I. Shein,<sup>18</sup> A. Shevel,<sup>41,48</sup> T.-A. Shibata,<sup>42,52</sup> K. Shigaki,<sup>17</sup> M. Shimomura,<sup>53</sup> K. Shoji,<sup>27,42</sup> A. Sickles,<sup>49</sup> C. L. Silva,<sup>46</sup> D. Silvermyr,<sup>38</sup> C. Silvestre,<sup>11</sup> K. S. Sim,<sup>25</sup> C. P. Singh,<sup>2</sup> V. Singh,<sup>2</sup> S. Skutnik,<sup>21</sup> M. Slunečka,<sup>5,22</sup> A. Soldatov,<sup>18</sup> R. A. Soltz,<sup>29</sup> W. E. Sondheim,<sup>30</sup> S. P. Sorensen,<sup>51</sup> I. V. Sourikova,<sup>3</sup> F. Staley,<sup>11</sup> P. W. Stankus,<sup>38</sup> E. Stenlund,<sup>32</sup> M. Stepanov,<sup>37</sup> A. Ster,<sup>24</sup> S. P. Stoll,<sup>3</sup> T. Sugitate,<sup>17</sup> C. Suire,<sup>39</sup> J. Sziklai,<sup>24</sup> T. Tabaru,<sup>43</sup> S. Takagi,<sup>53</sup> E. M. Takagui,<sup>46</sup> A. Taketani,<sup>42,43</sup> Y. Tanaka,<sup>35</sup> K. Tanida,<sup>42,43</sup> M. J. Tannenbaum,<sup>3</sup> A. Taranenko,<sup>48</sup> P. Tarján,<sup>12</sup> T. L. Thomas,<sup>36</sup> M. Togawa,<sup>27,42</sup> A. Toia,<sup>49</sup> J. Tojo,<sup>42</sup> L. Tomásek,<sup>20</sup> H. Torii,<sup>42</sup> R. S. Towell,<sup>1</sup> V.-N. Tram,<sup>28</sup> I. Tserruya,<sup>56</sup> Y. Tsuchimoto,<sup>17</sup> C. Vale,<sup>21</sup> H. Valle,<sup>54</sup> H. W. van Hecke,<sup>30</sup> J. Velkovska,<sup>54</sup> R. Vertesi,<sup>12</sup> A. A. Vinogradov,<sup>26</sup> M. Virius,<sup>10</sup> V. Vrba,<sup>20</sup> E. Vznuzdaev,<sup>41</sup> M. Wagner,<sup>27,42</sup> D. Walker,<sup>49</sup> X. R. Wang,<sup>37</sup> Y. Watanabe,<sup>42,43</sup> J. Wessels,<sup>33</sup> S. N. White,<sup>3</sup> D. Winter,<sup>9</sup> C. L. Woody,<sup>3</sup> M. Wysocki,<sup>8</sup> W. Xie,<sup>43</sup> Y. Yamaguchi,<sup>55</sup> A. Yanovich,<sup>18</sup> Z. Yasin,<sup>4</sup> J. Ying,<sup>16</sup> S. Yokkaichi,<sup>42,43</sup> G. R. Young,<sup>38</sup> I. Younus,<sup>36</sup> I. E. Yushmanov,<sup>26</sup> W. A. Zajc,<sup>9</sup> O. Zaudtke,<sup>33</sup> C. Zhang,<sup>38</sup> S. Zhou,<sup>6</sup> J. Zimányi,<sup>24,†</sup> and L. Zolin<sup>22</sup>

(PHENIX Collaboration)

- <sup>1</sup>Abilene Christian University, Abilene, Texas 79699, USA  
<sup>2</sup>Department of Physics, Banaras Hindu University, Varanasi 221005, India  
<sup>3</sup>Brookhaven National Laboratory, Upton, New York 11973-5000, USA  
<sup>4</sup>University of California, Riverside, Riverside, California 92521, USA  
<sup>5</sup>Charles University, Ovocný trh 5, Praha 1, 116 36 Prague, Czech Republic  
<sup>6</sup>China Institute of Atomic Energy (CIAE), Beijing, People's Republic of China  
<sup>7</sup>Center for Nuclear Study, Graduate School of Science, University of Tokyo, 7-3-1 Hongo, Bunkyo, Tokyo 113-0033, Japan  
<sup>8</sup>University of Colorado, Boulder, Colorado 80309, USA  
<sup>9</sup>Columbia University, New York, New York 10027, USA, and Nevis Laboratories, Irvington, New York 10533, USA  
<sup>10</sup>Czech Technical University, Zikova 4, Praha 6, 166 36 Prague, Czech Republic  
<sup>11</sup>Dapnia, CEA Saclay, F-91191 Gif-sur-Yvette, France  
<sup>12</sup>Debrecen University, H-4010 Debrecen, Egyetem tér 1, Hungary  
<sup>13</sup>ELTE, Eötvös Loránd University, H-1117 Budapest, Pázmány P. s. 1/A, Hungary  
<sup>14</sup>Florida Institute of Technology, Melbourne, Florida 32901, USA  
<sup>15</sup>Florida State University, Tallahassee, Florida 32306, USA  
<sup>16</sup>Georgia State University, Atlanta, Georgia 30303, USA  
<sup>17</sup>Hiroshima University, Kagamiyama, Higashi-Hiroshima 739-8526, Japan  
<sup>18</sup>IHEP Protvino, State Research Center of Russian Federation, Institute for High Energy Physics, Protvino 142281, Russia  
<sup>19</sup>University of Illinois at Urbana-Champaign, Urbana, Illinois 61801, USA  
<sup>20</sup>Institute of Physics, Academy of Sciences of the Czech Republic, Na Slovance 2, Praha 8, 182 21 Prague, Czech Republic  
<sup>21</sup>Iowa State University, Ames, Iowa 50011, USA  
<sup>22</sup>Joint Institute for Nuclear Research, 141980 Dubna, Moscow Region, Russia  
<sup>23</sup>KEK, High Energy Accelerator Research Organization, Tsukuba, Ibaraki 305-0801, Japan  
<sup>24</sup>KFKI Research Institute for Particle and Nuclear Physics of the Hungarian Academy of Sciences (MTA KFKI RMKI), H-1525 Budapest 114, P.O. Box 49, Budapest, Hungary  
<sup>25</sup>Korea University, Seoul, 136-701, Korea  
<sup>26</sup>Russian Research Center Kurchatov Institute, Moscow, Russia  
<sup>27</sup>Kyoto University, Kyoto 606-8502, Japan  
<sup>28</sup>Laboratoire Leprince-Ringuet, Ecole Polytechnique (CNRS-IN2P3), Route de Saclay, F-91128 Palaiseau, France  
<sup>29</sup>Lawrence Livermore National Laboratory, Livermore, California 94550, USA  
<sup>30</sup>Los Alamos National Laboratory, Los Alamos, New Mexico 87545, USA  
<sup>31</sup>LPC, Université Blaise Pascal (CNRS-IN2P3), Clermont-Fd, 63177 Aubiere Cedex, France  
<sup>32</sup>Department of Physics, Lund University, P.O. Box 118, SE-221 00 Lund, Sweden  
<sup>33</sup>Institut für Kernphysik, University of Muenster, D-48149 Muenster, Germany  
<sup>34</sup>Myongji University, Yongin, Kyonggido 449-728, Korea  
<sup>35</sup>Nagasaki Institute of Applied Science, Nagasaki-shi, Nagasaki 851-0193, Japan  
<sup>36</sup>University of New Mexico, Albuquerque, New Mexico 87131, USA  
<sup>37</sup>New Mexico State University, Las Cruces, New Mexico 88003, USA  
<sup>38</sup>Oak Ridge National Laboratory, Oak Ridge, Tennessee 37831, USA  
<sup>39</sup>IPN-Orsay, Université Paris Sud (CNRS-IN2P3), BP 1, F-91406 Orsay, France  
<sup>40</sup>Peking University, Beijing, People's Republic of China  
<sup>41</sup>Petersburg Nuclear Physics Institute (PNPI), Gatchina, Leningrad Region 188300, Russia  
<sup>42</sup>RIKEN, The Institute of Physical and Chemical Research, Wako, Saitama 351-0198, Japan  
<sup>43</sup>RIKEN BNL Research Center, Brookhaven National Laboratory, Upton, New York 11973-5000, USA  
<sup>44</sup>Physics Department, Rikkyo University, 3-34-1 Nishi-Ikebukuro, Toshima, Tokyo 171-8501, Japan  
<sup>45</sup>Saint Petersburg State Polytechnic University, St. Petersburg, Russia  
<sup>46</sup>Universidade de São Paulo, Instituto de Física, Caixa Postal 66318, São Paulo CEP05315-970, Brazil  
<sup>47</sup>System Electronics Laboratory, Seoul National University, Seoul, South Korea  
<sup>48</sup>Chemistry Department, Stony Brook University, SUNY, Stony Brook, New York 11794-3400, USA  
<sup>49</sup>Department of Physics and Astronomy, Stony Brook University, SUNY, Stony Brook, New York 11794-3800, USA  
<sup>50</sup>SUBATECH Ecole des Mines de Nantes (CNRS-IN2P3), Université de Nantes BP 20722 - 44307 Nantes, France  
<sup>51</sup>University of Tennessee, Knoxville, Tennessee 37996, USA  
<sup>52</sup>Department of Physics, Tokyo Institute of Technology, Oh-okayama, Meguro, Tokyo 152-8551, Japan  
<sup>53</sup>Institute of Physics, University of Tsukuba, Tsukuba, Ibaraki 305, Japan  
<sup>54</sup>Vanderbilt University, Nashville, Tennessee 37235, USA  
<sup>55</sup>Waseda University, Advanced Research Institute for Science and Engineering, 17 Kikui-cho, Shinjuku-ku, Tokyo 162-0044, Japan  
<sup>56</sup>Weizmann Institute, Rehovot 76100, Israel  
<sup>57</sup>Yonsei University, IPAP, Seoul 120-749, Korea

(Received 27 April 2007; published 25 September 2007)

\*PHENIX spokesperson: [jacak@skipper.physics.sunysb.edu](mailto:jacak@skipper.physics.sunysb.edu)

†Deceased

The PHENIX experiment presents results from the Relativistic Heavy Ion Collider 2005 run with polarized proton collisions at  $\sqrt{s} = 200$  GeV, for inclusive  $\pi^0$  production at midrapidity. Unpolarized cross section results are given for transverse momenta  $p_T = 0.5$  to 20 GeV/ $c$ , extending the range of published data to both lower and higher  $p_T$ . The cross section is described well for  $p_T < 1$  GeV/ $c$  by an exponential in  $p_T$ , and, for  $p_T > 2$  GeV/ $c$ , by perturbative QCD. Double helicity asymmetries  $A_{LL}$  are presented based on a factor of 5 improvement in uncertainties as compared to previously published results, due to both an improved beam polarization of 50%, and to higher integrated luminosity. These measurements are sensitive to the gluon polarization in the proton. Using one representative model of gluon polarization it is demonstrated that the gluon spin contribution to the proton spin is significantly constrained.

DOI: [10.1103/PhysRevD.76.051106](https://doi.org/10.1103/PhysRevD.76.051106)

PACS numbers: 13.85.Ni, 13.88.+e, 21.10.Hw, 25.40.Ep

A principal goal of the spin program at the Relativistic Heavy Ion Collider (RHIC) at Brookhaven National Laboratory is to determine the gluon spin contribution to a longitudinally polarized proton ( $\Delta G$ ), taking advantage of the strongly interacting probes available in proton-proton collisions [1]. Previous measurements have established the validity of the perturbative quantum chromodynamics (pQCD) description for inclusive midrapidity  $\pi^0$  [2] and forward  $\pi^0$  production [3], and for midrapidity jet [4] and direct photon production [5], at  $\sqrt{s} = 200$  GeV. The double helicity asymmetries for the production of these particles involve gluons in the hard scattering processes in this pQCD description, and the first measurements for  $\pi^0$  [6,7] and for jets [4] have begun to probe  $\Delta G$ .

The RHIC beam polarization and luminosity have significantly improved [8]. The statistical uncertainty for a double helicity asymmetry measurement is proportional to the inverse of  $P^2 \times \sqrt{\mathcal{L}}$  for beam polarizations  $P$  and integrated luminosity  $\mathcal{L}$ , and decreased by a factor of 5 from the previously published data from PHENIX [6,7].

In this paper, we first present the cross section for midrapidity  $\pi^0$  production for unpolarized proton-proton collisions at  $\sqrt{s} = 200$  GeV. These results extend to lower and higher  $p_T$  than in previous publications, and we discuss an apparent transition region between soft and hard scattering; the inclusive cross section is dominated by hard scattering, described by pQCD, for  $p_T > 2$  GeV/ $c$ . We then present the double helicity asymmetry,  $A_{LL}$ , for midrapidity  $\pi^0$  production. We also include measurements of  $A_{LL}$  at low  $p_T$ , below the hard scattering region. Finally, our results for  $p_T > 2$  GeV/ $c$  are compared to a pQCD calculation that incorporates a model of gluon polarization. We present the range that we probe in the gluon momentum fraction ( $x_g$ ) and discuss the constraint from these data on  $\Delta G$ .

The PHENIX experiment at RHIC measured  $\pi^0$ 's via  $\pi^0 \rightarrow \gamma\gamma$  decays using a highly segmented ( $\Delta\eta \times \Delta\phi \sim 0.01 \times 0.01$ ) electromagnetic calorimeter (EMCal) [9], covering a pseudorapidity range of  $|\eta| < 0.35$  and azimuthal angle range of  $\Delta\phi = \pi$ . The  $\pi^0$  data in this analysis were collected using two different trigger conditions. A minimum bias (MB) trigger was defined by the coincidence of signals in two beam-beam counters (BBC) with

full azimuthal coverage located at pseudorapidities  $\pm(3.0 - 3.9)$  [10]. The cross section for events selected by the MB trigger was 23.0 mb (about half of  $\sigma_{pp}^{\text{inel}}$ ) with a systematic uncertainty of  $\pm 9.7\%$ , derived from vernier scan results [2] and the variation of MB trigger efficiency for subsequent years. Higher  $p_T$  data were collected using the coincidence of the MB trigger and an EMCal-based high  $p_T$  photon trigger [2,11], with efficiency  $\sim 5\%$  at  $p_T(\pi^0) \sim 1$  GeV/ $c$  and  $\sim 90\%$  for  $p_T(\pi^0) > 3.5$  GeV/ $c$ . The collision vertex was required to be within  $|z| < 30$  cm along the beam axis, based on the time difference between the two BBC detectors. The  $\pi^0$  acceptance is uniform over this interval. The analyzed data sample of the 2005 run corresponds to an integrated luminosity of  $2.5 \text{ pb}^{-1}$ .

Details of the unpolarized cross section analysis technique are described in [2,11]. The background contribution under the  $\pi^0$  peak in the two-photon invariant mass distribution varied from 80% in the lowest 0.5–0.75 GeV/ $c$   $p_T$  bin to less than 8% for  $p_T > 4$  GeV/ $c$ . The  $\pi^0$  spectrum was corrected for overlapping decay photon showers in the EMCal, based on Monte Carlo simulations confirmed with test beam data [12]. Below a  $p_T(\pi^0)$  of 12 GeV/ $c$  the correction is less than 4%, and for  $p_T(\pi^0) = 20$  GeV/ $c$  the correction is  $\sim 25\%$  and  $\sim 70\%$ , for two different EMCal subsystems [9]. The systematic uncertainty of the measurement (excluding the 9.7% uncertainty from the MB trigger cross section) varied from  $\sim 7\%$  at  $p_T \sim 1$  GeV/ $c$  to  $\sim 16\%$  for the highest  $p_T$  bin.

Figure 1 presents the cross section results for midrapidity  $\pi^0$  production at  $\sqrt{s} = 200$  GeV, versus  $p_T$ , from  $p_T = 0.5$  GeV/ $c$  to  $p_T = 20$  GeV [13]. Points are plotted at the average  $p_T$  for each bin. The pQCD prediction, at next-to-leading order (NLO), is shown for theory scales  $\mu = p_T/2$ ,  $p_T$  and  $2p_T$ , where  $\mu$  represents equal factorization, renormalization, and fragmentation scales [14,15]. The Coordinated Theoretical-Experimental Project on QCD (CTEQ6M) parton distribution functions [16] and Kniehl-Kramer-Pötter set of fragmentation functions [17] are used. These data extend the published cross section data at both low and high  $p_T$ , and are consistent with previously published results [2,11]. From  $p_T = 2$  GeV/ $c$  to 20 GeV/ $c$ , the NLO pQCD calculation describes the data over a change in cross section of 7 orders of magni-

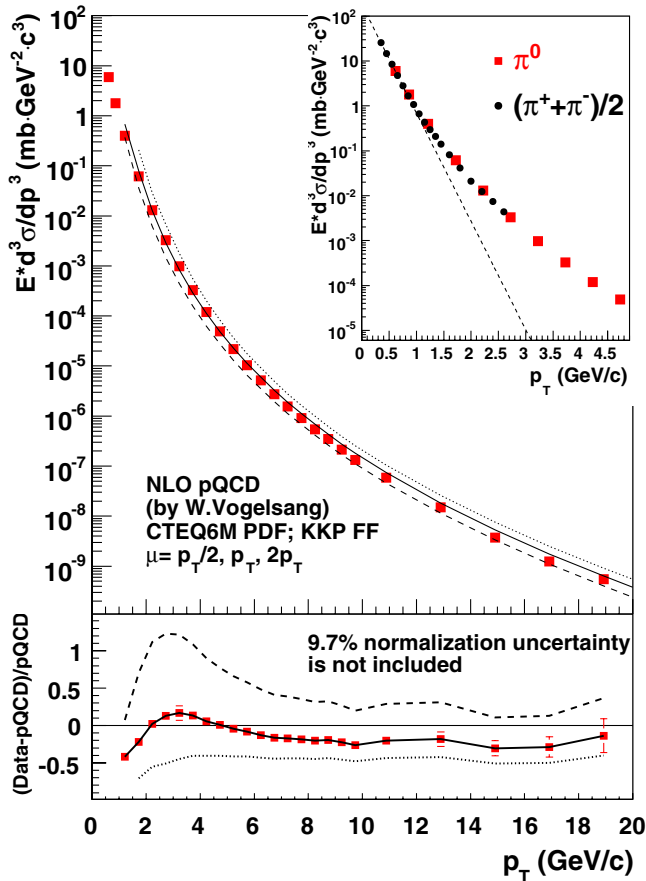


FIG. 1 (color online). The neutral pion production cross section at  $\sqrt{s} = 200$  GeV as a function of  $p_T$  (squares) and the results of NLO pQCD calculations for theory scales  $\mu = p_T/2$  (dotted line),  $p_T$  (solid line) and  $2p_T$  (dashed line), see text for details; note that the error bars are smaller than the points. The inset shows, in addition to  $\pi^0$  (squares), data for  $(\pi^+ + \pi^-)/2$  (solid circles), and a fit of charged pion data to an exponential function for  $p_T < 0.8$  GeV/ $c$  (dashed line). The bottom panel shows the relative difference between the data and theory for the three theory scales. Experimental uncertainties (excluding the 9.7% normalization uncertainty) are shown for the  $\mu = p_T$  curve.

tude. We note also more recent theoretical work which describes the RHIC midrapidity  $\pi^0$  data, and which introduces an intrinsic  $k_T$  dependence into the parton distribution and fragmentation functions [18], or which includes soft gluon emission in the interaction [19]. Both new approaches improve agreement with data at lower energies and have a smaller effect on the  $\sqrt{s} = 200$  GeV midrapidity cross sections.

The inset of Fig. 1 shows the lower  $p_T$  region in more detail including high precision data for the charged pion cross section from [20]. The data show a transition in the  $p_T$  dependence of the cross section, from exponential to a power law dependence, in the region  $p_T \approx 1$ – $2$  GeV/ $c$ . In order to estimate possible contamination from nonperturbative physics in the higher  $p_T$  data, an exponential func-

tion ( $\sim e^{-\alpha p_T}$ ) representing a nonperturbative component is fit to the charged pion spectrum in the region  $p_T = 0.3$  to  $0.8$  GeV/ $c$  (only the lowest  $p_T$   $\pi^0$  data point is in this range) and extrapolated to the higher  $p_T$  region. The exponential fit for the low  $p_T$  region gives  $\alpha = 5.56 \pm 0.02$  (GeV/ $c$ ) $^{-1}$ , with  $\chi^2/NDF = 6.2/3$ . Only statistical uncertainties for the charged pion data were used in the fit. The dominant systematic uncertainty for the points in the fitted  $p_T$  range is a  $\sim 12\%$  normalization uncertainty (excluding the normalization uncertainty from the MB trigger cross section). Beyond about  $p_T = 1$  GeV/ $c$ , the data lie above this single exponential. The fraction of the exponential contribution to the data for the 2–2.5 GeV/ $c$   $p_T$  bin is found to be less than 10%, with a negligible contribution for higher  $p_T$ . This is the basis for applying the pQCD formalism to the double helicity asymmetry data with  $p_T > 2$  GeV/ $c$ .

For the 2005 run, each collider ring of RHIC was filled with up to 111 bunches in a 120 bunch pattern, spaced 106 ns apart, with predetermined patterns of polarization signs for the bunches. Spin rotators, sets of four helical dipole magnets on each side of PHENIX, rotate the polarization orientation from vertical, the stable spin direction in the RHIC arcs, to longitudinal at the interaction point [21]. Beam helicity asymmetries are obtained by tagging the polarization signs of the bunches for each event. The bunches for one beam alternate in polarization sign, and pairs of bunches alternate in sign for the other beam. In this way data for all combinations of beam helicity are collected at the same time, and the possibility of false asymmetries due to changing detector response versus spin state is greatly reduced. Each RHIC fill, typically lasting 8 h, used one of four bunch spin patterns.

The beam polarizations for 2005 were measured using fast carbon target polarimeters [22], normalized by absolute polarization measurements made during 2005 by a separate polarized atomic hydrogen jet polarimeter [23]. The beam polarizations, from luminosity-weighted averages over 104 RHIC fills used in the analysis, were  $\langle P^B \rangle = 0.50 \pm 0.002(\text{stat}) \pm 0.025(\text{systB}) \pm 0.015(\text{systG})$  and  $\langle P^Y \rangle = 0.49 \pm 0.002(\text{stat}) \pm 0.025(\text{systY}) \pm 0.015(\text{systG})$ , for blue ( $B$ ) and yellow ( $Y$ ) RHIC beams, respectively, for the bunches colliding at PHENIX. The systematic uncertainties have been separated into uncorrelated uncertainties for each beam, “systB” and “systY,” and a global systematic uncertainty “systG,” which is common for both beams and comes from systematic uncertainty in jet polarimeter measurements [24]. For comparison, the polarizations in the 2004 run were  $0.44 \pm 0.08(\text{syst})$ .

Local polarimeters based on very forward neutron production (production angle 0.3–2.5 mrad) [6,25] were used to set up and monitor the beam polarization orientation at PHENIX. The polarimeters monitor the transverse polarization of each beam at PHENIX, which can be compared to the beam polarization measured by the RHIC polar-

imeters where the polarization direction is vertical. The local polarimeters were calibrated by turning off the spin rotators around PHENIX, and measuring the response of the local polarimeters with the beams vertically polarized. For the longitudinal polarization data, the beams showed a measurable transverse polarization, with  $(P_T/P)^B = 0.10 \pm 0.02$  and  $(P_T/P)^Y = 0.14 \pm 0.02$ , with  $P_T/P$  referring to the fraction of transverse polarization of each beam. The polarization directions, as determined by the spin rotator settings and as measured by the local polarimeters, remained constant over the run. The product of the beam polarizations  $P^B \cdot P^Y$  is required for the double helicity asymmetry measurement. The average transverse component of the product was  $\langle P_T^B \cdot P_T^Y \rangle / \langle P^B \cdot P^Y \rangle < (P_T/P)^B \cdot (P_T/P)^Y = 0.014 \pm 0.003$ ; the average of the polarization product over the run was  $\langle P^B \cdot P^Y \rangle = 0.24$  with a systematic uncertainty of  $\pm 9.4\%$ .

The double helicity asymmetry  $A_{LL}$  is the difference of cross sections for the same versus opposite beam helicities, divided by the sum. Experimentally, for inclusive  $\pi^0$  production, it can be determined as

$$A_{LL}^{\pi^0} = \frac{1}{|P^B \cdot P^Y|} \cdot \frac{N_{++} - R \cdot N_{+-}}{N_{++} + R \cdot N_{+-}}; \quad R = \frac{L_{++}}{L_{+-}}, \quad (1)$$

where  $N$  is the number of  $\pi^0$ 's measured in PHENIX from the colliding bunches with the same ( $++$ ) and opposite ( $+-$ ) helicities, and  $R$  is the relative luminosity between bunches with the same and opposite helicities. Here we neglect the parity-violating difference in cross section between  $(++) \leftrightarrow (--)$  and  $(+-) \leftrightarrow (-+)$  beam helicity configurations [26].  $A_{LL}$  was calculated for each fill in order to reduce systematics from variation in beam polarizations and in  $R$  for different fills. Even and odd crossings were handled by separate high  $p_T$  photon trigger electronics chains. To avoid possible detector bias,  $A_{LL}$  was also determined separately for the even and odd crossings. Final asymmetries were averaged, and corrected for the asymmetry of the background under the  $\pi^0$  peak in the two-photon mass distribution  $A_{LL}^{BG}$ , measured from the data outside the  $\pi^0$  peak region (50 MeV/ $c^2$  wide bands on either side of the  $\pi^0$  peak) [6].  $A_{LL}^{BG}$  was consistent with zero in all  $p_T$  bins.

The relative luminosity ratio  $R$  is obtained from the MB triggers discussed above. Scalers keep track of the number of live triggers for each bunch crossing. Single beam background was  $< 0.05\%$ , as measured from noncolliding bunches, and contributes negligible systematic uncertainty to the measured  $R$ . We also measured the double helicity asymmetry of the relative luminosity scaler counts, by normalizing using zero degree neutral particle production as measured by zero degree calorimeters (ZDC) [27]. No asymmetry was observed. This gave a limit on an asymmetry bias in the measurement of  $\delta A_{LL}^{\pi^0}|_{\text{bias}} < 2 \times 10^{-4}$ , and a limit on the systematic uncertainty for the measurement of relative luminosity giving  $\delta A_{LL}^{\pi^0}|_R < 2 \times 10^{-4}$ .

These limits also include the effects from the pileup of two or more collisions in a crossing, calculated at  $\leq 4\%$  of the crossings. The BBC and ZDC monitors observe the pileup at significantly different rates, and therefore the limits above, from comparing BBC and ZDC counts, include these uncertainties.

A transverse double spin asymmetry  $A_{TT}$ , the transverse equivalent to Eq. (1), can contribute to  $A_{LL}$  through the 1.4% transverse component of the product of the beam polarizations discussed above. Although  $A_{TT}$  has been postulated to be extremely small,  $\sim 10^{-4}$  [28], it has not been previously measured. We measured  $A_{TT}$  in a short run with transverse polarization.  $A_{TT}(p_T)$  was consistent with zero within statistical errors [13]; the errors were 5 times larger than the uncertainties for  $A_{LL}$ ,  $\delta^{\text{stat}} A_{LL}$ . Therefore, a limit was determined for the  $A_{TT}$  contribution to  $A_{LL}$  of  $0.07 \cdot \delta^{\text{stat}} A_{LL}$ .

Figure 2 presents the measured double helicity asymmetry in  $\pi^0$  production [13]. A scale uncertainty of 9.4% in  $A_{LL}^{\pi^0}$  due to the uncertainty in beam polarization is not shown. The other systematic uncertainties are negligible, as discussed above, and checked using a bunch polarization sign randomization technique, and by varying the  $\pi^0$  identification criteria [6]. Data for  $p_T > 1$  GeV/ $c$  were obtained from the high  $p_T$  photon triggered sample. For  $p_T$  below 1 GeV/ $c$ , due to low efficiency for the high  $p_T$  photon trigger, we used the MB data sample. In the low  $p_T$  region, where the cross section shows an exponential

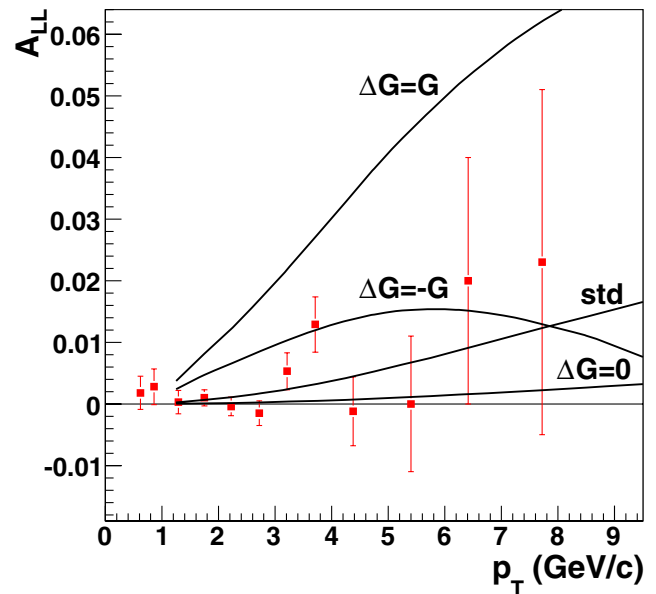


FIG. 2 (color online). The double helicity asymmetry for neutral pion production at  $\sqrt{s} = 200$  GeV as a function of  $p_T$  (GeV/ $c$ ). Error bars are statistical uncertainties, with the 9.4% scale uncertainty not shown; other experimental systematic uncertainties are negligible. Four GRSV theoretical calculations based on NLO pQCD are also shown for comparison with the data (see text for details).

A. ADARE *et al.*

behavior, the helicity asymmetry is  $A_{LL}^{\pi^0} = 0.002 \pm 0.002$ , for the data in the range  $p_T = 0.5 - 1$  GeV/c. For the higher  $p_T$  region, the four curves in Fig. 2 show calculations of  $A_{LL}^{\pi^0}$ , using NLO pQCD with  $\mu = p_T(\pi^0)$ , that reflect the range of gluon polarizations allowed by inclusive deep inelastic scattering (DIS) data. The calculations are based on the Glück-Reya-Stratmann-Vogelsang (GRSV) model, where “standard” (std) was the best fit to inclusive DIS data [29]. For momentum fraction  $x$ ,  $\Delta G(x) = G^+(x) - G^-(x)$  refers to the gluon helicity distribution, and  $G^+(x)$  and  $G^-(x)$  refer to the gluon densities for + and - helicities in a + helicity proton. The first moment of the gluon helicity distribution,  $\int_0^1 \Delta G(x) dx$ , for the std parameterization is  $\Delta G = 0.4$ , at the scale  $Q^2 = 1$  GeV<sup>2</sup>. The other three curves are calculations based on this best fit, but use at  $Q^2 = 0.4$  GeV<sup>2</sup> the function  $\Delta G(x) = G(x)$ , 0,  $-G(x)$ , where  $G(x)$  is the unpolarized gluon distribution. The gluon distribution at the input scale is evolved to the scale  $Q^2 = p_T^2(\pi^0)$ .

In order to explore the impact of the new data on the sensitivity to the polarized gluon distribution, we have compared the data with a set of  $A_{LL}(p_T)$  curves corresponding to different  $\Delta G(x)$  between  $\Delta G(x) = -G(x)$  and  $\Delta G(x) = G(x)$  at  $Q^2 = 0.4$  GeV<sup>2</sup>. We used the data for  $p_T > 2$  GeV/c, which appear to have little contamination from soft physics as discussed earlier.

Combining the estimate of the soft physics fraction in the  $p_T = 2-2.5$  GeV/c bin of  $<10\%$ , with the soft physics asymmetry as measured for  $p_T < 1$  GeV/c, a soft physics contribution to the asymmetry in the  $p_T = 2 - 2.5$  GeV/c bin would be  $\lesssim 2 \cdot 10^{-4}$ , and negligible for higher  $p_T$  bins. We note, however, that a parton intrinsic  $k_T$  [18] could still affect the lower  $p_T$  asymmetries, for  $p_T \approx 2-3$  GeV/c, and this is not addressed in the GRSV model.

The most likely  $x_g$  for PHENIX  $\pi^0$  data in each  $p_T$  point is  $\sim x_T/0.7$  [30], where  $x_T = p_T/(\sqrt{s}/2)$ . For the measured  $p_T$  range 2–9 GeV/c, the range of  $x_g$  in each bin is broad, and spans the range  $x_g = 0.02-0.3$ , as calculated by NLO pQCD [31].

Figure 3 shows the corresponding  $\chi^2$  versus  $\Delta G_{\text{GRSV}}^{x=[0.02 \rightarrow 0.3]}$ , where we compare to an integral of  $\Delta G$  over the probed  $x_g$  range. Only experimental statistical uncertainties are used to calculate  $\chi^2$ , and no theoretical uncertainties are included. It is important to note, that although the range of the first moment explored represents  $\sim 60\%$  of the full integral, this reflects using a specific model for the gluon polarization. For example, a gluon polarization model with a crossover from positive to negative gluon polarization within our  $x_g$  range would yield a small average asymmetry for each point. Also, other models can generate larger or smaller contributions from the gluon spin in the unmeasured region of  $x_g$ .

These data are sensitive to the first moment of the polarized gluon distribution. Using the GRSV model, we find that the gluon polarization contribution to the proton

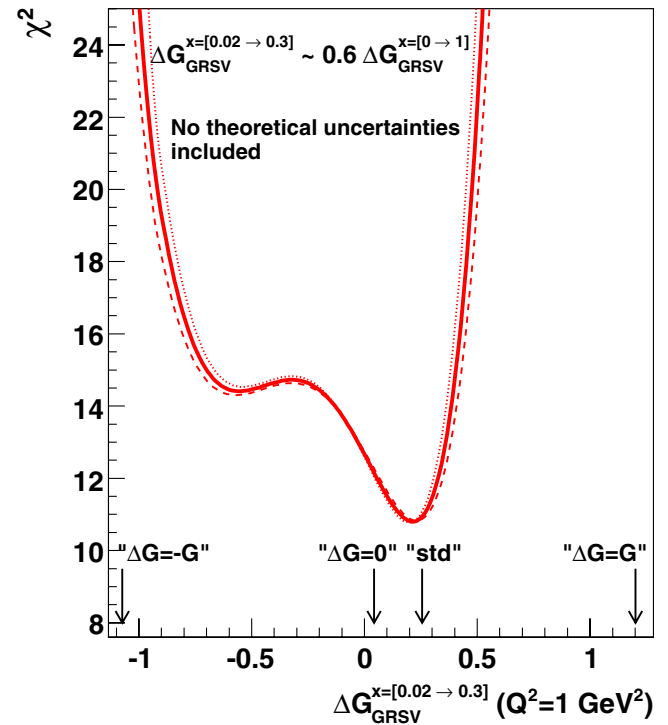


FIG. 3 (color online). The  $\chi^2$  distribution of the measured data plotted versus the value of the first moment of the polarized gluon distribution (solid line) in the  $x_g$  range from 0.02 to 0.3 corresponding to our  $\pi^0$  data in  $p_T$  bins from 2 to 9 GeV/c. Dashed and dotted lines correspond to  $-9.4\%$  and  $+9.4\%$  variation in  $A_{LL}$  normalization related to the beam polarization uncertainty, the dominant systematic uncertainty of our data. Only statistical uncertainties were used for each curve. Arrows indicate  $\Delta G$  corresponding to the different polarized gluon distributions discussed in the text.

spin (1/2) in the probed  $x_g$  range is constrained between  $-0.9$  and  $+0.5$ , for  $\chi^2 - \chi_{\min}^2 = 9$ , representing a “ $3\sigma$ ” limit (a “ $1\sigma$ ” limit would give a constraint between 0.07 and 0.3). The extremes of gluon polarization are ruled out, modulo the above remarks, with the confidence level for “ $\Delta G = \pm G$ ” of less than  $10^{-6}$ . Large positive gluon polarization [32] was proposed shortly after the discovery that the quark contribution to the proton spin was small [33], with the suggestion that such a large gluon polarization would mask a “bare” quark polarization. For std and “ $\Delta G = 0$ ”, the confidence levels are 20%–21% and 12%–13%, respectively, for the range of  $\pm 9.4\%$  scale uncertainty of the measurement. Semi-inclusive DIS measurements [34] have also presented data on  $\Delta G$  in a limited  $x_g$  range and its comparison with various  $\Delta G$  scenarios.

The two minima in Fig. 3 reflect the quadratic contribution of the gluon polarization to  $A_{LL}$ , from the gluon-gluon scattering subprocess for  $\pi^0$  production. The symmetry between the two minima is broken by the quark-gluon scattering subprocess, where the gluon polarization contributes linearly to  $A_{LL}$ . The quark-gluon subprocess is emphasized at higher  $p_T$ , which will become accessible

with additional running at high polarization and luminosity.

To summarize, we have presented the unpolarized cross section and double helicity asymmetries for  $\pi^0$  production at midrapidity, for proton-proton collisions at  $\sqrt{s} = 200$  GeV. We observe an apparent transition region in the cross section, for  $p_T \approx 1$  to 2 GeV/ $c$ , with the cross section described by an exponential in  $p_T$  below  $p_T \sim 1$  GeV/ $c$ , and with the cross section described by the pQCD prediction for  $p_T = 2$  to 20 GeV/ $c$ , over 7 orders of magnitude in cross section. The results for  $A_{LL}$  in the pQCD region, which we take as  $p_T \geq 2$  GeV/ $c$ , constrain the gluon polarization in the proton significantly. The range probed is  $x_g = 0.02$  to 0.3, for the gluon momentum fraction. Using one representative model for the gluon polarization, GRSV [29], which assumes no crossover in gluon polarization versus  $x_g$ , we present a map of  $\chi^2$  versus the first moment of the polarized gluon distribution in the measured region. From this study, the present data rule

out extreme values of gluon polarization suggested after the surprise of the EMC result that the quarks (and anti-quarks) contribute little to the spin of the proton [33], but allow significant contribution from the gluon spin to the proton spin.

We thank the RHIC Polarimeter Group and the staff of the Collider-Accelerator and Physics Departments at BNL for their vital contributions. We thank W. Vogelsang and M. Stratmann for providing the NLO pQCD calculations and for informative discussions. We acknowledge support from the Department of Energy and NSF (USA), MEXT, and JSPS (Japan), CNPq and FAPESP (Brazil), NSFC (China), MSMT (Czech Republic), IN2P3/CNRS, and CEA (France), BMBF, DAAD, and AvH (Germany), OTKA (Hungary), DAE (India), ISF (Israel), KRF and KOSEF (Korea), MES, RAS, and FAE (Russia), VR and KAW (Sweden), U.S. CRDF for the FSU, USA-Hungarian NSF-OTKA-MTA, and USA-Israel BSF.

- 
- [1] G. Bunce *et al.*, *Annu. Rev. Nucl. Part. Sci.* **50**, 525 (2000).
- [2] S. S. Adler *et al.*, *Phys. Rev. Lett.* **91**, 241803 (2003).
- [3] J. Adams *et al.*, *Phys. Rev. Lett.* **92**, 171801 (2004).
- [4] B. I. Abelev *et al.*, *Phys. Rev. Lett.* **97**, 252001 (2006).
- [5] S. S. Adler *et al.*, *Phys. Rev. Lett.* **98**, 012002 (2007).
- [6] S. S. Adler *et al.*, *Phys. Rev. Lett.* **93**, 202002 (2004).
- [7] S. S. Adler *et al.*, *Phys. Rev. D* **73**, 091102 (2006).
- [8] M. Bai *et al.*, *Proceedings of the 2005 Particle Accelerator Conference*, edited by C. Horak (IEEE, New York, 2005), p. 600.
- [9] L. Aphecetche *et al.*, *Nucl. Instrum. Methods Phys. Res., Sect. A* **499**, 521 (2003).
- [10] M. Allen *et al.*, *Nucl. Instrum. Methods Phys. Res., Sect. A* **499**, 549 (2003).
- [11] S. S. Adler *et al.*, *Phys. Rev. Lett.* **98**, 172302 (2007).
- [12] G. David *et al.*, *IEEE Trans. Nucl. Sci.* **47**, 1982 (2000).
- [13] Tables of data available at [http://www.phenix.bnl.gov/phenix/WWW/info/data/ppg063\\_data.html](http://www.phenix.bnl.gov/phenix/WWW/info/data/ppg063_data.html)
- [14] F. Aversa *et al.*, *Nucl. Phys.* **B327**, 105 (1989).
- [15] B. Jäger *et al.*, *Phys. Rev. D* **67**, 054005 (2003).
- [16] J. Pumplin *et al.*, *J. High Energy Phys.* **07** (2002) 012.
- [17] B. A. Kniehl, G. Kramer, and B. Pötter, *Nucl. Phys.* **B597**, 337 (2001).
- [18] U. D'Alesio and F. Murgia, *Phys. Rev. D* **70**, 074009 (2004).
- [19] D. de Florian and W. Vogelsang, *Phys. Rev. D* **71**, 114004 (2005).
- [20] S. S. Adler *et al.*, *Phys. Rev. C* **74**, 024904 (2006).
- [21] W. W. MacKay *et al.*, *Proceedings of the 2003 Particle Accelerator Conference*, edited by J. Chew, P. Lucas, and S. Webber (IEEE, Portland, OR, 2003), p. 1697.
- [22] O. Jinnouchi *et al.*, *RHIC/CAD Accelerator Physics Note* 171, 2004.
- [23] H. Okada *et al.*, *Phys. Lett. B* **638**, 450 (2006).
- [24] I. Nakagawa *et al.*, *RHIC/CAD Accelerator Physics Note* 275, 2007; O. Eyster *et al.*, *RHIC/CAD Accelerator Physics Note* 274 (2007).
- [25] Y. Fukao *et al.*, *Phys. Lett. B* **650**, 325 (2007).
- [26] PHENIX has measured parity-violating single helicity asymmetry  $A_L$  for each polarized beam, which was consistent with zero within statistical uncertainty, in all  $p_T$  bins [6,13].
- [27] C. Adler *et al.*, *Nucl. Instrum. Methods Phys. Res., Sect. A* **470**, 488 (2001).
- [28] A. Mukherjee *et al.*, *Phys. Rev. D* **72**, 034011 (2005).
- [29] B. Jäger, A. Schäfer, M. Stratmann, and W. Vogelsang, *Phys. Rev. D* **67**, 054005 (2003); M. Glück, E. Reya, M. Stratmann, and W. Vogelsang, *Phys. Rev. D* **63**, 094005 (2001).
- [30] S. S. Adler *et al.*, *Phys. Rev. D* **74**, 072002 (2006).
- [31] M. Stratmann and W. Vogelsang, arXiv:hep-ph/0702083; W. Vogelsang (private communication).
- [32] G. Altarelli and G. Ross, *Phys. Lett. B* **212**, 391 (1988); G. Altarelli and W. J. Stirling, *Part. World* **1**, 40 (1989); R. D. Carlitz, J. C. Collins, and A. H. Mueller, *Phys. Lett. B* **214**, 229 (1988).
- [33] J. Ashman *et al.* (EMC Collaboration), *Phys. Lett. B* **206**, 364 (1988); *J. Nucl. Phys.* **B328**, 1 (1989).
- [34] B. Adeva *et al.* (SMC Collaboration), *Phys. Rev. D* **70**, 012002 (2004); E. S. Ageev *et al.* (COMPASS Collaboration), *Phys. Lett. B* **633**, 25 (2006); A. Airapetian *et al.* (HERMES Collaboration), *Phys. Rev. Lett.* **84**, 2584 (2000).